Development of Granular Catalysts and Natural Gas Combustion Technology for Small Gas Turbine Power Plants

Zinfer R. Ismagilov[1], Mikhail A. Kerzhentsev[1], Svetlana A. Yashnik[1],
Nadezhda V. Shikina[1], Andrei N. Zagoruiko[1], Valentin N. Parmon[1],
Vladimir M. Zakharov[2], Boris I. Braynin[2] and Oleg N. Favorski[2]
[1]Boreskov Institute of Catalysis, 630090, Novosibirsk
[2]Central Institute of Aviation Motors, Moscow
Russia

1. Introduction

Gas turbine power plants (GTPPs) of low power (tens of kW to 1.5-2 MW) are promising autonomous sources of energy and heat. The application of gas turbine technologies saves fuel, solves heat supply and water shortage problems. The nominal efficiency of GTTPs belonging to different generations varies from 24% to 38% (average weighted efficiency – 29%). This is 1.5 times higher than that of combined heat power plants.

The main GTPP drawback is significant emission of toxic nitrogen oxides due to high temperature combustion of the gas fuel. The main approach used today to decrease the emission of nitrogen oxides from GTPPs is based on the use of the so-called homogeneous combustion chambers working with premixed lean fuel-air mixtures with two-fold excess of air. The decrease of NO_x formation is principally the result of the low flame temperatures that are encountered under lean conditions (Correa 1992). This technology makes it possible to decrease significantly the temperature in the combustion zone relative to traditional GTPP combustion chambers with separate supply of fuel and air to the combustion zone. As a result, the concentration of nitrogen oxides in the flue gases decreases from 100 ppm to 10-20 ppm. The downside of this approach is, however, that it results in low heat release rates, which, in turn, may negatively affect combustion stability.

The most efficient way to decrease emissions of nitrogen oxides in GTPPs is to use catalytic combustion of fuel (Trimm, 1983; Pfefferle & Pfeferle., 1987; Ismagilov & Kerzhentsev 1990; Parmon et al., 1992; Ismagilov et al., 1995; Ismagilov & Kerzhentsev, 1999; Ismagilov et al., 2010). In the catalytic chamber, efficient combustion of homogeneous fuel-air mixture is achieved at larger excess of air and much lower temperatures in the zone of chemical reactions compared to modern homogeneous combustion chambers.

In the last decade, the obvious advantages of the catalytic combustion chambers in GTPPs initiated intense scientific and applied studies in the USA (Catalytica) and Japan (Kawasaki Heavy Industries) which are aimed at development of such chambers for GTPPs for various applications (Dalla Betta et al., 1995; Dalla Betta & Tsurumi, 1995; Dalla Betta & Rostrup-Nielsen, 1999; Dalla Betta & Velasco, 2002).

The catalyst in a gas-turbine combustor has to withstand continuous operation for at least 10,000 h under severe operation conditions: high gas hourly space velocity (GHSV) and temperatures over 1200 K (McCarty et al., 1999). Material development is therefore one of the key issues in the development of catalytic combustion for gas turbines. Such catalyst has to possess high mechanical strength and the ability to initiate methane oxidation in lean mixtures at low temperatures 620-720 K and maintain stable oxidation during long time at temperatures above 1200 K (Dalla Betta et al., 1995; Dalla Betta & Rostrup-Nielsen, 1999).

Today catalysts for gas turbines are prepared in the form of monoliths from foil made of special corrosion-resistant alloys with deposited porous support and the active component based on platinum and/or palladium (Dalla Betta et al., 1995a; McCarty et al. 2000; Carroni et al. 2003). However, application of such catalysts requires many problems to be solved. The main problems are related to the high temperature of gas typical for modern gas turbines that requires the catalyst to operate at temperatures exceeding 1200 K for prolonged periods of time (total operation time of modern GTPPs reaches 100000 hours) (McCarty et al., 1999). The use of metal supports at temperatures above 900°C is limited due to possible thermal corrosion, especially in the presence of water vapor. It results in the catalyst destruction, peeling of the support and loss of noble metals decreasing the catalytic activity and shortening the catalyst lifetime. So, the improvement of the catalyst stability is an urgent problem.

One of the approaches to solve this problem is based on development of catalysts on granulated supports and design of a catalytic package for GTPP combustion chamber, which would provide minimum emissions of NO_x, CO and HC at moderate temperatures (930-950°C). In this chapter we present our results on development and study of alternative granular catalysts with reduced Pd content for methane catalytic combustion in mini gas turbines of 400-500 kW power with regenerative cycle, intended for decentralized power supply. The small power of these turbines results in reduced catalyst loading and makes possible the use of granular catalysts which are less expensive and can be easily manufactured using existing industrial facilities.

2. Selection of catalysts for application in gas turbine combustors

The most available fuel for GTPPs is natural gas, which consists largely of methane, which is the least readily oxidizable hydrocarbon. Therefore, it is necessary to produce catalysts capable of initiating methane oxidation at minimum possible temperatures and withstanding long-term exposure to temperatures above 930°C.

It is very difficult to find catalysts meeting requirements of both high activity at low temperature and good thermal stability at high temperatures. Therefore, in catalytic gas combustors generally staged combustion is employed: a highly reactive catalyst for the low-temperature (350 °C < T_{in} < 450 °C) conversion of CH_4 must be combined with a second catalyst which converts fuel at higher temperatures (T_{in} approx. 700 °C, T_{out} > 900 °C) (Carroni et al. 2002).

It is well known that catalysts based on noble metals are most active in oxidation reactions. They can initiate combustion at low temperatures, but it is inappropriate to use them above 750°C because of a high volatility of the noble metals (Arai et al. 1986). Use of palladium as the active component in the high-temperature oxidation of methane is most promising. This is because palladium has a high specific activity in this reaction (Burch & Hayes, 1995; Lee & Trimm, 1995) and a relatively low volatility in comparison with other noble metals, as was

determined by studying the interaction of the metals with oxygen at 730–1730°C (McCarty et al., 1999). It is these properties of palladium that attract researchers' interest to its behavior in the methane oxidation reaction. It is well known that, up to 800° C, palladium exists as PdO_x which undergoes reduction to palladium metal as the temperature is further raised. This reaction is reversible up to ca. 900°C, so a decrease in temperature leads to the reoxidation of Pd to PdO_x in air. As a consequence, the temperature dependence of the methane conversion always shows a hysteresis (Farrauto et al., 1992). There is still no consensus as to what form of oxidized palladium — bulk PdO, Pd with oxygen chemisorbed on its surface, or Pd particles covered by PdO — is the most active species in combustion ((McCarty, 1995; Burch, 1996; Su et al., 1998a; Su et al., 1998 b; Lyubovsky & Pfefferle, 1998; Lyubovsky & Pfefferle, 1999).

Supporting of palladium on a substrate, primarily γ- or α-Al_2O_3 or Al_2O_3 modified with rare-earth metal oxides, raises the activity and thermal stability of the catalyst through an increase in the degree of dispersion of the active component and in its aggregation stability (Baldwin & Burch, 1990; Groppi et al., 1999, Ismagilov et al., 2003, Ozawa et al., 2003, Liotta & Deganello, 2003; Yue et al., 2005).

Alternative catalytic systems for methane combustion are catalysts based on hexaaluminates and transition metal oxides. Hexaaluminates are the class of compounds with a general formula $AB_xAl_{12-x}O_{19}$, where A is a rare-earth or alkaline-earth metal, such as La and Ba, and B is a transition metal with an atomic radius comparable to the radius of aluminum (B = Mn, Co, Fe, Cr, Ni) (Machida et al., 1987; Machida et al., 1989). Hexaaluminates form from oxides at temperatures above 1200°C, and this is why they are very stable up to high temperatures. The specific surface area of hexaaluminates and, accordingly, their activity in methane oxidation depend on the preparation method (Chouldhary et al., 2002). However, irrespective of their specific surface area, the hexaaluminates are much less active than the palladium catalysts. In view of this, there have been attempts to enhance the catalytic activity of hexaaluminates by introducing Pd (Jang et al., 1999). In our earlier work (Yashnik et al. 2006), it was shown that introducing 0.5 wt % Pd into the hexaaluminate $(Mn,Mg)LaAl_{11}O_{19}$ resulted in a significant increase in the catalyst activity expressed as a 110°C decrease in the temperature of 50% methane conversion ($T_{50\%}$). In addition, a synergistic effect in the Pd–$(Mn,Mg)LaA_{11}O_{19}$ system was detected.

It was demonstrated earlier that thermally stable catalysts could be prepared from manganese oxides (Tsikoza et al., 2002; Tsikoza et al., 2003). The activity of these catalysts in hydrocarbon oxidation can be enhanced by their calcination at 900–1100°C. In our works (Tsikoza et al., 2002; Tsikoza et al., 2003), it was found that Mn–Al–O catalysts supported on γ-Al_2O_3 containing χ-Al_2O_3 and modified with Mg, La, or Ce were more active and thermally more stable (up to 1300°C) than the same catalysts supported on pure γ-Al_2O_3. We believe that the high degree of disorder of the χ-Al_2O_3 structure in comparison with γ-Al_2O_3 favors deeper interaction of manganese and modifiers with the support at the impregnation and low-temperature calcination stages. This yields Mn–Al–O compounds of complex composition (solid solutions and/or hexaaluminates) at 1300°C, due to which the catalysts are stable and highly active in methane oxidation.

Thus, based on literature data and our research results, two types of catalysts were selected for further development and study: (1) active Pd catalysts with low ignition temperature for initiation of methane combustion and (2) thermally stable hexaaluminate catalysts for methane combustion at temperatures over 900°C.

3. Synthesis of granular catalysts for methane combustion

3.1 Preparation of catalysts

In catalyst preparation, we used γ-alumina supports developed at the Boreskov Institute of Catalysis (Shepeleva et al., 1991; Ismagilov et al., 1991, Koryabkina et al., 1991; Koryabkina et al., 1996) prepared in the form of spheres and rings. Their characteristics are presented in Table 1.

Property	Spherical Al_2O_3	Ring-shaped Al_2O_3
Diameter, mm	2.2–2.5	7.5
Length, mm	-	7.5
Inner diameter, mm	-	2.5
Bulk density, g/cm³	0.8	0.7
Pore volume (H_2O), cm³/g	0.45	0.45
Specific surface area, m²/g	180	200
Crushing strength under static conditions, kg/cm²	270	23
Phase composition	γ-Al_2O_3	60% γ-Al_2O_3 40% χ-Al_2O_3

Table 1. Physicochemical properties of the spherical and ring-shaped aluminas

Pd–Ce–Al₂O₃. The catalyst was prepared on the ring-shaped support and contained 12 wt %CeO₂ and 2 wt % Pd. It was prepared by the incipient-wetness impregnation of the support with a cerium nitrate (Ce(NO₃)₃ · 6H₂O) solution and then with an aqueous Pd(NO₃)₂ solution. Before being loaded with palladium, the alumina support modified with cerium was calcined at 600°C. After supporting of palladium, it was additionally calcined at 1000°C. The pilot catalyst batch was designated IK-12-60-2.

Mn–Al₂O₃.The catalyst was prepared on the ring-shaped support by the incipient wetness impregnation of the support with an aqueous manganese nitrate (Mn(NO₃)₂* 6H₂O) solution. It contained 11 wt % manganese oxides in terms of MnO₂. The catalyst calcination temperature was 900°C. It was similar in composition to the commercial catalyst IKT-12-40; for this reason, its pilot batch is hereafter designated IKT-12-40A.

Mn-La–Al₂O₃. This catalyst was prepared on the ring-shaped support by successive incipient-wetness impregnation of alumina with lanthanum and manganese nitrate solutions using the procedure described in (Yashnik et al., 2006). It contained 8–11 wt % manganese in terms of MnO₂ and 10–12 wt % lanthanum in terms of La₂O₃. These concentrations of manganese and lanthanum are sufficient to ensure a high catalytic activity and stability of the catalyst (Yashnik et al., 2006). The calcination temperature was 1000°C, lower than the temperature used in our previous study (Yashnik et al., 2006) and was equal to the onset temperature of hexaaluminate phase formation. This allowed us to increase the specific surface area of the sample. The pilot catalyst batch was designated IK-12-61.

Pd–Mn–La–Al₂O₃. This catalyst was prepared on the ring-shaped support by successive incipient-wetness impregnation with lanthanum and manganese nitrate solutions. Next, the samples were dried and calcined at 400°C. Thereafter, the samples were loaded with a palladium nitrate solution by impregnation. Final calcination was carried out at 1000°C. The resulting catalyst contained 8–11 wt % Mn in terms of MnO₂, 10–12 wt % La in terms of La₂O₃, and was 0.65 wt % Pd. The pilot batch of the catalyst was designated IK-12-62-2.

3.2 Characterization of catalysts

When developing and optimizing the catalysts based on manganese oxides, including those additionally containing lanthanum and palladium, we investigated how their physicochemical and catalytic properties depend on their chemical composition, the active component and modifier (manganese, lanthanum, palladium, and hexaaluminate phase) contents, the chemical nature of Mn and Pd precursors, the calcination temperature, and the active component introduction method (Yashnik et al., 2006; Tsikoza et al., 2002; Tsikoza et al., 2003). Measuring the catalytic activity of catalyst samples in methane oxidation allowed us to find the optimal catalytic systems, whose properties are listed in Table 2.

The catalysts on the ring-shaped alumina support (IK-12-60-2, IKT-12-40A, IK-12-61, IK-12-62-2) were tested in natural gas combustion at 930°C in the pilot plant at the Boreskov Institute of Catalysis.

The results of these tests are presented in Table 3. The catalyst IK-12-60-2 retained its high activity over 100 h: the ignition temperature (T_{ign}) was 240°C, and the reaction products were almost free of CO and NO_x. The manganese-containing catalysts were less active: with these catalysts, T_{ign} and the residual CO and NO_x contents were higher than with IK-12-60-2. However, the initial activity of the catalyst IK-12-61 did not decrease, but even gradually increased during testing: in 200 h, T_{ign} falls from 365 to 350°C, the NO_x concentration in the reaction products remained at the 0–1 ppm level, and the CO concentration decreased from 55 to 34 ppm. The catalyst IK-12-61 modified with 0.65 wt % palladium (IK-12-62-2) allowed us to reduce the ignition temperature of the methane–air mixture almost by 100°C and the CO concentration in the reaction products by more than one order of magnitude. Service life tests suggested that all catalysts are tolerant to high temperatures (up to 930°C) and to the action of the reaction medium. The ignition temperature and the methane–air combustion efficiency remained unchanged at least over 100 h of testing.

The investigation of the physicochemical properties of the initial samples (Table 2) showed that, in IK-12-60-2, the active component PdO is finely dispersed and this allows one to initiate combustion of the methane–air mixture at low temperatures.

The initial catalysts based on Mn and La oxides (IK-12-61 and IK-12-62-2) contain the hexaaluminate phase, which is known to be resistant to high temperatures. The durability tests altered the structural and textural characteristics of the catalysts (Table 4). Over the first 50 h of testing, the specific surface area and pore volume of the IK-12-60-2 catalyst decreased because of the coarsening of alumina particles and the onset of α-Al_2O_3 formation via the δ-Al_2O_3 – α-Al_2O_3 phase transition under prolonged heating. The active component PdO underwent partial decomposition to Pd^0. In the next 50 h, the textural parameters stabilized and the degree of dispersion of the remaining PdO phase increased. The degree of dispersion of metallic Pd^0 decreased with testing time. The Mn catalysts are more tolerant to high temperatures and are less prone to aggregation than the Pd–Ce catalyst. Some changes in the phase composition of the catalysts occur because of the formation of high-temperature phases, namely, α-Al_2O_3 and a (Mn, Al)Al_2O_4 solid solution in IKT-12-40A and manganese hexaaluminate in IK-12-61 and IK-12-62-2.

The catalytic activity of the hexaaluminate-based samples in the CH_4 oxidation reaction after 100-h-long testing was similar to the activity of the fresh catalysts: T_{50} is 470–480°C for the catalyst IK-12-61 and 363–380°C for IK-12-62-2 at GHSV = 1000 h^{-1} (Fig. 1). The activity of the catalysts Pd–Ce–Al_2O_3 and MnO_x–Al_2O_3 decreased slightly, and T_{50} increased by 50°C.

Catalyst	Calci-nation tempe-rature, °C	Chemical compo-sition, wt %	Phase composition*	S_{sp},** m^2/g	V_Σ (N_{ads})***, cm^3/g	Strength, kg/cm^2	$T_{, 50\%}$ $_{CH_4}$,**** °C
IK-12-60-2	1000	Pd – 2.1 Ce – 10.1	δ-Al_2O_3, CeO_2 (~200 Å, S_{33}=1100), PdO (~180 and 250 Å, S_{39} = 480)	74	0.26	24	330
IKT-12-40A	900	Mn – 6.9	Mixture of (δ + γ)-Al_2O_3, α-Al_2O_3, Mn_2O_3	80	0.23	23	400
IK-12-61	1000	Mn – 6.9 La – 10.1	$MnLaAl_{11}O_{19}$ (S_{37} = 60), $LaAlO_3$, γ-Al_2O_3#	43	0.18	34	420
IK-12-62-2	1000	Pd – 0.65 Mn – 7.1 La – 9.4	$MnLaAl_{11}O_{19}$ (S_{37} – traces),γ-Al_2O_3 (a = 7.937 A),PdO (~400 A, S_{39} = 70)	48	-	25	385

*The particle size was derived from the size of coherent-scattering domain region. Relative phase contents were estimated from peak areas (S_i, arb.units) in diffraction patterns. γ-Al_2O_3# is a solid solution based on γ-Al_2O_3. ** S_{sp} is specific surface area, ***V_Σ (N_{ads}) is pore volume found form N_2 adsorption, ****$T_{, 50\% CH_4}$ is temperature of 50% methane conversion on catalyst fraction 0.5-1.0 mm at GHSV = 1000 h^{-1} and methane concentration in air equal to 1%.

Table 2. Physicochemical and catalytic properties of the initial catalysts on spherical and ring-shaped supports

Catalyst	Test duration, h	T_{ign} , °C	Residual content, ppm	
			CO	NO_x
IK-12-60-2	100	240	0-1	0-1
IKT-12-40A	100	350	84-55	0-1
IK-12-61	200	365-350	55-34	0-1
IK-12-62-2	200	290	2-3	0-1

Table 3. Results of catalyst durability tests in natural gas combustion at 930°C in a bench testing unit at the Boreskov Institute of Catalysis

The catalytic activity of the hexaaluminate-based samples in the CH_4 oxidation reaction after 100-h-long testing was similar to the activity of the fresh catalysts: T_{50} is 470–480°C for the catalyst IK-12-61 and 363–380°C for IK-12-62-2 at GHSV = 1000 h^{-1} (Fig. 1). The activity of the catalysts Pd–Ce–Al_2O_3 and MnO_x–Al_2O_3 decreased slightly, and T_{50} increased by 50°C.

Catalyst	Test duration, h	Phase composition	S_{sp}, m²/g	V_Σ (N$_{ads}$), cm³/g	Strength, kg/cm²
IK-12-60-2	50	δ-Al$_2$O$_3$, α-Al$_2$O$_3$ (traces), CeO$_2$ (~200 Å, S_{33} = 1100), PdO (~ 300 Å, S_{39} = 180), Pd^o (~ 300 Å, S_{47} = 120)	42	0.18	21
	100	δ-Al$_2$O$_3$, α-Al$_2$O$_3$ (traces), CeO$_2$ (~200 Å, S_{33} = 1100), PdO (~ 160 Å, S_{39} = 180), Pd^o (~500 Å, S_{47} = 80)	38	0.17	19
IKT-12-40A	100	α-Al$_2$O$_3$, γ-Al$_2$O$_3$-based solid solution (Mn, Al)Al$_2$O$_4$ (a = 8.151 Å)	66	0.22	19
IK-12-61	30	MnLaAl$_{11}$O$_{19}$ (S_{37} = 240), LaAlO$_3$, α-Al$_2$O$_3$	41	0.18	30
	50	MnLaAl$_{11}$O$_{19}$ (S_{37} = 250), LaAlO$_3$, α-Al$_2$O$_3$	33	0.15	28
	100	MnLaAl$_{11}$O$_{19}$ (S_{37} = 240), LaAlO$_3$, α-Al$_2$O$_3$	31	0.13	28
IK-12-62-2	50	MnLaAl$_{11}$O$_{19}$ (S_{37} = 230), γ-Al$_2$O$_3$# (a = 7.937 Å), Pd^o (S_{41} = 90), PdO (400 Å, S_{39} = 160)	31	-	29
	100	MnLaAl$_{11}$O$_{19}$ (S_{37} = 230), γ-Al$_2$O$_3$# (a = 7.937 Å), Pd^o (>400 Å, S_{47} = 40), PdO (>400 Å, S_{39} = 160)	30	-	32
	200	MnLaAl$_{11}$O$_{19}$ (S_{37} = 340), γ-Al$_2$O$_3$# (a = 7.937 Å), α-Al$_2$O$_3$ (S_{29} = 30), PdO (>400 Å, S_{39} = 180), Pd^o (>400 Å, S_{47} = 40)	30	-	35

Table 4. Physicochemical properties of the catalysts after durability tests in natural gas combustion
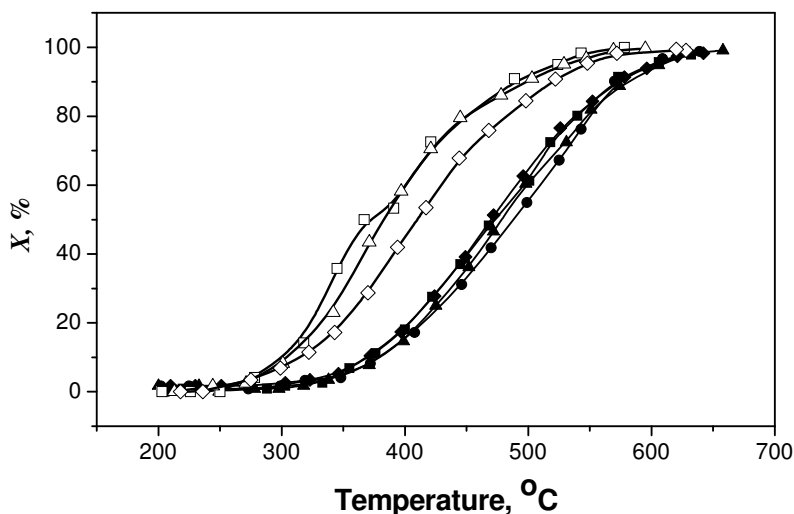
Fig. 1. Temperature dependences of methane conversion (1 vol % CH_4 in air, GHSV=1000 h^{-1}) on the catalysts: IK-12-61: ▲ – initial; ●-after 30 h; ■ - after 50 h; ◆ - after 100 h testing in CH_4 combustion at 930°C; IK-12-62-2: △- initial; □- after 50 h; ◊- after 100 h testing.

4. Kinetic studies of methane catalytic oxidation

Kinetic studies of methane catalytic oxidation were performed in a flow reactor. The reaction order with respect to methane was found to be equal to 1. In kinetic calculations, we used activity data for the 0.5–1.0 mm size fractions of the catalysts in methane oxidation at GHSV = 1000, 24000, and 48000 h^{-1}. The results obtained by data processing in the plug flow approximation are presented in Table 5. The obtained kinetic parameters were used further for modeling of methane combustion.

Catalyst	k_0, s^{-1}	E, kJ/mol
IK-12-60-2	4.36×10^7	81.4
IKT-12-40A	1.09×10^5	71.2
IK-12-61	1.09×10^5	71.2
IK-12-62-2	3.29×10^5	63.8

Table 5. Kinetic parameters of the total methane oxidation reaction

5. Experimental studies of natural gas combustion in a catalytic combustion chamber

5.1 Experimental procedures
Experimental studies of natural gas combustion were carried out in a stainless-steel tubular vertical catalytic combustion chamber (CCC) with an internal diameter of 80 mm. The CCC is schematically shown in Fig. 2. The volume of the catalytic package was 1.3 L.
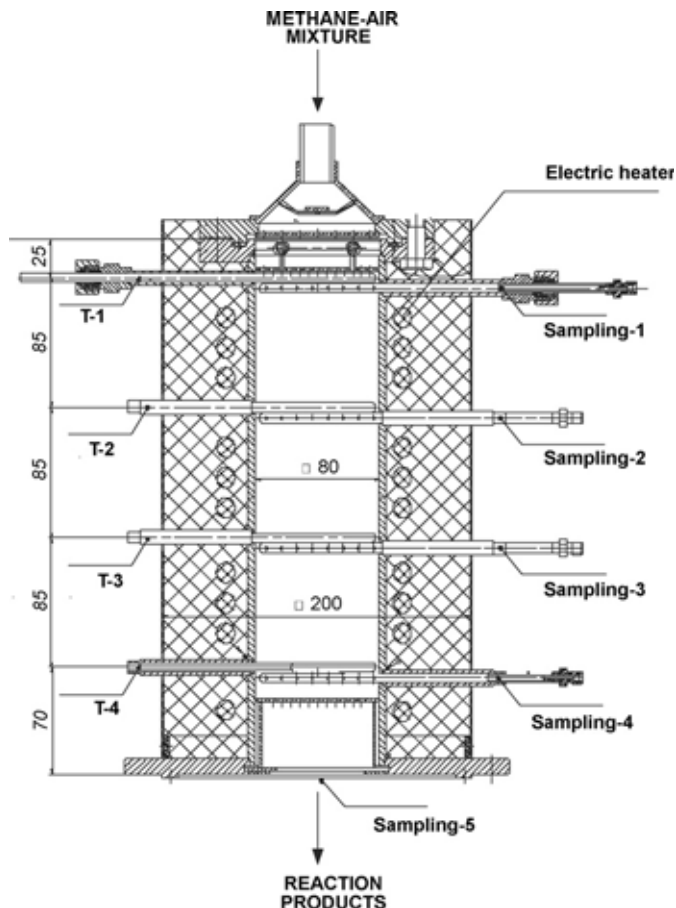
Fig. 2. Schematic view of the catalytic combustion chamber: T-1 to T-4: thermocouples,
sampling 1–5: gas samplers.

The air/fuel equivalence ratio (α) was selected to be close to the minimum value of this
parameter in the operating regime of full-power GTPP (α= 6.4–6.8). The inlet temperature of
the fuel–air mixture (T_{in}) was varied between 470 and 600°C, the temperature at the chamber
exit (T_{ex}) was 900–985°C, the GHSV of the fuel–air mixture was 8500–15,000 h^{-1}.

Natural gas was introduced into the combustion chamber after reaching the light-off
temperature. Due to the natural gas combustion, the temperature in the catalyst bed
increased and reached the values close to the desired ones in 30–40 min. The temperature
mode was corrected by smooth variation of the air and natural gas flows.

When the desired temperature regime was reached, temperatures along the length of the
catalytic chamber were measured. The radial temperature profile was measured before and
after the pilot-plant tests. A reference manometer was used to measure the pressures in the
catalyst bed. The gas phase composition at the CCC outlet was analyzed using a "Kristall-
2000 M" gas chromatograph. The gas probes were also analyzed in parallel using ECOM-AC
gas analyzer.

The catalytic packages studied are schematically presented in Fig. 3.

1. uniform loading with ring shaped high temperature resistant oxide catalyst
2. two high temperature catalysts with different granule shape. According to the results of modeling, the methane conversion should increase with change of granule shape as: ring < cylinder < sphere. However, the use of spherical catalyst for entire reactor is impossible due to a high pressure drop. Therefore, the reactor consists of two sections: the first with ring shaped oxide catalyst (or Pd-Mn-Al-O) and the second downstream section with spherical catalyst having lower fractional void volume. This combination with a short bed of spherical catalyst provides rather high methane combustion efficiency at a minor increase of pressure drop.
3. two ring shaped catalysts with different catalytic activity. In this case, a short bed (ca.10%) of the highly active Pd-Ce-catalyst is located in the upstream section at low temperature, and it initiates methane combustion. The larger bed of high temperature resistant oxide catalyst in the downstream section provides high efficiency of methane combustion. This design of catalytic reactor allows a reduction of total Pd loading and an increase of methane combustion efficiency at a low inlet temperature.
4. three catalysts with different catalytic activity and fractional void volume. The highly active Pd-catalyst in the upstream section initiates methane oxidation, the high temperature resistant catalyst in the larger middle section provides stable methane combustion. The bicomponent spherical Pd-Mn-Al-O catalyst with a low Pd-content and low fractional void volume in the downstream section improves the efficiency regarding the residual traces.
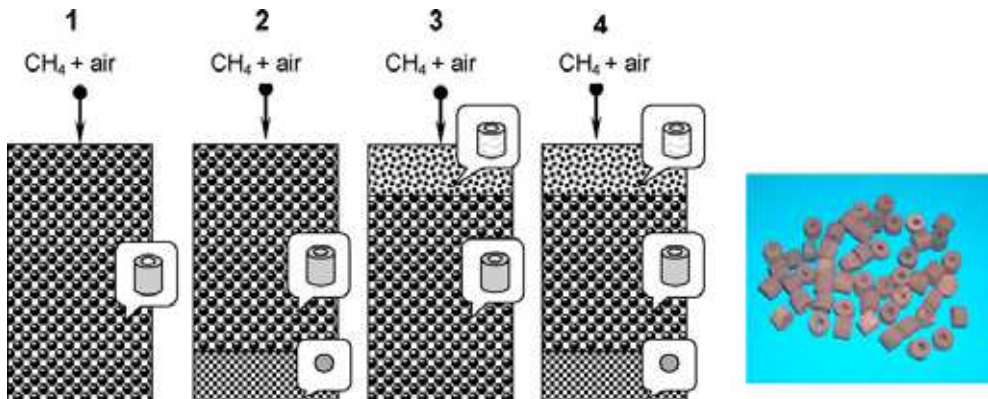
Fig. 3. Schemes of uniform (1) and structured (2–4) loading of the reactor and photo of granulated catalyst (Yashnik et al., 2009, Ismagilov et al., 2010)

5.2 Tests of the catalytic combustion chamber with uniform catalyst package

First, we tested CCC loaded with one catalyst. Such loading will be hereafter denoted as "uniform" and provides for one-stage combustion of the natural gas–air mixture. Such experiments allowed us to analyze the perspectives of using manganese–alumina catalysts and evaluate their catalytic properties in natural gas combustion by such parameters as outlet temperature and emission of hydrocarbons. $Mn–Al_2O_3$, $Mn–La–Al_2O_3$ and $Pd–Mn–La–Al_2O_3$ catalysts shaped as rings were tested for 72–120 h in a temperature cycle mode.

The temperature cycle mode consisted of four cycles of gas combustion, catalyst cooling and repeated start of the combustion process. The combustion process was carried out at GHSV= 15,000 h^{-1} and inlet temperature 580–600 $^\circ$C. The value of α was maintained at 6.8–6.9. The height of the catalytic package was 300 mm. The dynamics of changes in the activity of different catalysts are presented in Fig. 4.
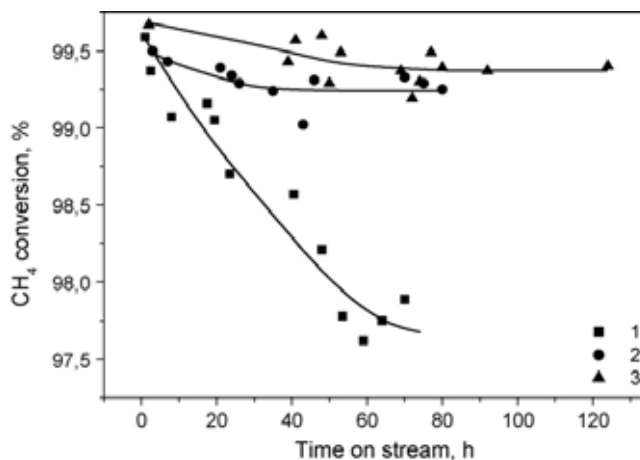
Fig. 4. Methane conversion vs. operation time in CCC at GHSV: 14,900–15,100 h^{-1} and α = 6.7–6.8. Uniform catalyst package loaded with: (1) Mn–Al$_2$O$_3$ (T$_{in}$ – 600 °C); (2) Mn–La–Al$_2$O$_3$ (T$_{in}$ – 600 °C); (3) Pd–Mn–La–Al$_2$O$_3$ (T$_{in}$ – 575–580 °C).

The data presented in Fig. 4 indicate that the catalysts Mn–Al$_2$O$_3$, Mn–La–Al$_2$O$_3$ and Pd–Mn–La–Al$_2$O$_3$ differ both by their activity and stability. For example, the activity of the Mn–Al$_2$O$_3$ catalyst gradually decreased as evidenced by gradual increase of the methane and CO concentration at the CCC outlet. The methane conversion decreased from 99.6% to 97.9% during the first 50–54 h on stream. Then the catalyst activity stabilized and did not change in the following 80 h on stream (Fig. 4, curve 1). At the end of the experiment the methane and CO concentrations stabilized at 330 and 110 ppm, respectively (Table 6).

Table 6 compares the outlet temperatures and emissions of CH$_4$ and CO during natural gas combustion over Mn–Al$_2$O$_3$ catalysts with different fractional compositions at GHSV= 8500–15,000 h^{-1}.It was shown that the methane combustion efficiency over large catalyst granules with the external ring diameter 15mm was low.

Even at a low load on the catalyst (GHSV = 8500 h^{-1}) the methane conversion was 97% whereas the methane and CO emissions at the outlet were 500 and 300 ppm, respectively. Note that under similar CCC operation conditions the application of catalyst granules with the external diameter 7.5 mm allowed for a 10-fold decrease of the methane emission and 30-fold decrease of the CO emission. In both cases the CCC efficiency also depended on contact time. The contact time increase from 0.24 s (GHSV = 15,000 h^{-1}) to 0.42 s (GHSV = 8500 h^{-1}) affected more significantly the efficiency of CCC loaded with the catalyst with smaller internal and external diameters of the granules (7.5 mm), i.e. lower fractional void volume of the catalyst bed. These data indicate that the mass transfer of the reagents and reaction products to/from the catalyst surface substantially affects the total CCC efficiency in methane combustion at the inlet temperature 600 $^\circ$C. At this temperature methane

oxidation proceeds mainly on the catalyst surface and the contribution of homogeneous reactions is negligible, which is confirmed by substantial improvement of methane conversion with the increase of the catalysts geometrical surface.

These data agree with the work (Hayashi et al., 1995) where the authors showed the dependences of relative contributions of heterogeneous and homogeneous methane oxidation reactions on the monolithic Pt–Pd catalyst on the inlet temperature, pressure and the catalyst channel density. Placing the catalysts with small cells (200 cpsi) in the front part of the reactor allowed the increase of heat release there at 600 °C (Hayashi et al., 1995), at the same time in the monolith with larger channels (100 cpsi), especially at temperature 700 °C the homogeneous oxidation reaction was prevailing.

Frac-tion, mm	G_{air}, m³/h	G_{NG}, l/h	GHSV, h⁻¹	α	T_{in} °C	T_1* °C	T_2* °C	T_3* °C	T_4* °C	C_{CH4}, ppm	C_{CO}, ppm	C_{NOx} ppm	X_{CH4} %
7.5	19.4	309	14900	6.78	577	659	867	920	917	328	102	1	97.89
7.5	15.0	243	11500	6.70	567	677	903	926	905	164	41	2	98.68
7.5	11.1	180	8500	6.67	571	728	923	925	896	48	9	1	99.69
15	19.2	324	14800	6.41	590	623	763	898	918	987	943	1	93.87
15	15.0	267	11500	6.10	570	604	783	909	919	630	616	2	96.28
15	11.1	204	8500	5.90	562	591	790	903	897	504	344	2	97.13

G_{air} is volume flow rate of air, G_{GN} is volume flow rate of natural gas, C_{CH4}, C_{CO}, C_{NOx} are outlet concentrations of CH_4, CO and NO$_x$; X_{CH4} is methane conversion, *temperatures measured by thermocouples placed along the catalyst bed at different distances from the CCC inlet: T_1 – 25 mm; T_2 – 110 mm; T_3 – 195 mm; T_4 – 280 mm.

Table 6. Parameters of methane combustion over Mn-Al$_2$O$_3$ catalysts with different fractional composition

The activity of Mn–La–Al$_2$O$_3$ and Pd–Mn–La–Al$_2$O$_3$ catalysts also decreased in the first 30–40 h on stream. However, the activity decrease was less dramatic compared to the Mn–Al$_2$O$_3$ catalyst (Fig. 4). The methane conversion over Mn–La–Al$_2$O$_3$ and Pd–Mn–La–Al$_2$O$_3$ catalysts decreased from 99.5% to 99.3% (Fig. 4, curve 2) and from 99.7% to 99.4% (Fig. 4, curve 3), respectively. The concentrations of methane and CO stabilized at 100 and 85 ppm, correspondingly. Note that the Pd–Mn–La–Al$_2$O$_3$ catalyst showed these values of the residual CH_4 and CO concentrations at a lower inlet temperature 575 °C than the Mn–La–Al$_2$O$_3$ catalyst that showed similar values at 600 °C inlet temperature. The NO$_x$ concentration at the outlet of the catalyst package did not exceed 0–2 ppm on all the catalysts. Thus, the obtained results demonstrate that the activity of the Pd–Mn–La–Al$_2$O$_3$ catalyst was higher than that of the catalysts without Pd. Meanwhile, the stability of this catalyst was comparable to that of Mn–La–Al$_2$O$_3$ being determined by the Mn–hexaaluminate phase. The stability of these catalysts was much higher than that of the catalyst based on Mn oxide. These results of the catalysts testing under the above conditions are in good agreement with our results on the study of the catalysts activity in methane oxidation in a laboratory reactor (Yashnik et al., 2006; Tsikoza et al., 2002; Tsikoza et al., 2003). It was shown that modification of Mn-alumina catalysts with oxides of rare earth metals allowed a considerable increase of thermal stability of the catalysts due to the

formation of manganese–hexaaluminate phase (Yashnik et al., 2006; Tsikoza et al., 2002). Introduction of 0.5 wt.% Pd into Mn–La–Al$_2$O$_3$ resulted in a substantial decrease of the light-off temperature of the air–natural gas mixture (Yashnik et al., 2006).

The pressure drop on the full height of the catalyst bed for uniform loading of the catalysts in the form of 7.5 mm × 7.5 mm × 2.5 mm rings for the catalysts Mn–Al$_2$O$_3$, Mn–La–Al$_2$O$_3$ and Pd–Mn–La–Al$_2$O$_3$ was 35, 23 and 14 mbar at GHSV= 14,900, 11,500 and 8500 h^{-1}, respectively. These values are less 4% of the total pressure which was 1 bar.

Figure 5 shows the effect of the air/fuel equivalence ratio on the outlet temperature and methane conversion over the catalyst package loaded with the Mn–La–Al$_2$O$_3$ catalyst. The variation of α between 6.2 and 7.2 showed that its decrease (enrichment of the fuel–air mixture with methane) resulted in a growth of the temperature at the outlet of the catalyst bed and, consequently, increase of the methane conversion. For instance, when α was decreased from 7 to 6.2, the methane conversion increased from 99.3% to 99.93% and the temperature grew from 937 to 992 °C at GHSV= 15,000 h^{-1}. However, Fig. 5 shows that methane conversion above 99.9% was observed when the temperature in the catalyst bed exceeded 980°C. So high temperature is undesirable because the catalyst overheating during prolonged operation will inevitably lead to its deactivation. Therefore, alternative methods of increasing the methane conversion are required.

As it is known from the literature, one of the ways to increase the CCC efficiency is to use multistage (multizone) combustion. This method allows one to control the temperature profile by varying the catalyst activity in different zones of the catalytic combustion chamber. Several methods for stepwise combustion of hydrocarbon fuels in the GTPP CCC have been implemented. American companies Catalytica (Dalla Betta & Tsurumi, 1993) and Westinghouse Electric Corp. (Young & Carl, 1989) suggested feeding the fuel–air mixture to a monolith catalyst consisting of alternating channels with an active component and without it. If the surface reaction in the channel with a catalyst takes place in the diffusion-controlled regime, adiabatic heating to the flame temperature does not occur because the heat is transferred to the inert channel of the monolith. The fuel–air mixture exiting the inert channels is burnt at the exit of the monolith catalyst.
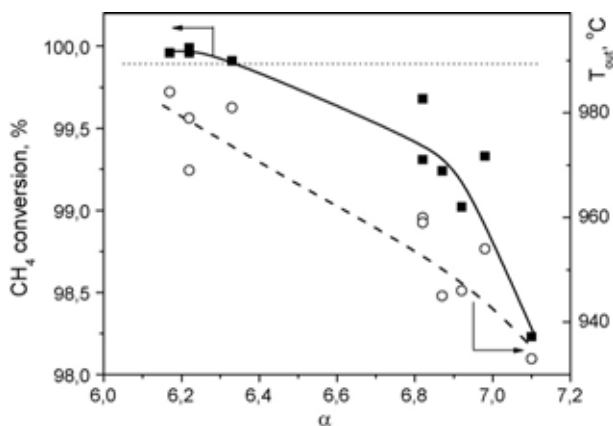
Fig. 5. Dependence of methane conversion (filled symbols) and catalyst temperature at the CCC outlet (open symbols) during methane combustion in CCC loaded with Mn–La–Al$_2$O$_3$ catalyst on α. GHSV= 15,000 h^{-1}, T$_{in}$ = 600 °C.

In patents (Dalla Betta & Tsurumi, 1993; Pfefferle, 1997) it was suggested to use multi-section catalysts with different levels of activity to carry out combustion in the kinetically controlled regime. The catalytic activity is regulated by varying the concentration of the noble metal (most often Pd) in the range of 5–20 wt.% or the nature of the active component (noble metal, transition metal oxides). It was also suggested (Dalla Betta & Velasco, 2002) to use a two-stage monolithic catalyst combined from catalytic systems with different thermal stabilities. A catalyst with low ignition temperature requiring minimal heating is placed at the entrance zone whereas a catalyst resistant to the action of high temperatures is placed at the exit.

5.3 Tests of CCC with combined two-stage catalyst package

We suggested a design of a two-stage catalyst package consisting of catalysts with the same chemical composition but different fractional compositions. Using the Pd–Mn–La–Al$_2$O$_3$ catalyst as an example we studied the effect of the catalyst bed fractional void volume on the methane conversion in CCC. The main part of the catalyst package was loaded with the catalyst formed as 7.5 mm × 7.5 mm × 2.5 mm rings having the fractional void volume (ε) 0.52. A catalyst layer with 60 mm height consisting of 4–5 mm spherical granules with fractional void volume 0.42 was placed near the outlet of the package. The total Pd concentration in the catalyst package was 0.6 wt.%.

The application of the spherical catalyst at the CCC outlet made it possible to achieve over 99.9% combustion efficiency (Fig. 6) and decrease the methane concentration from 85 ppm to 0–5mm and the CO concentration to 4–8 ppm at inlet temperature 580°C and α in the range of 6.7–7.1. Fig. 7 presents the methane and CO profiles along the reactor length. One can see that more than 90% of methane is oxidized at the distance ca. 200 mm from the inlet. The maximum CO concentration is observed in this region. Further combustion of methane and CO to concentrations below 10 ppm is observed mostly at 280–340 mm from the inlet of
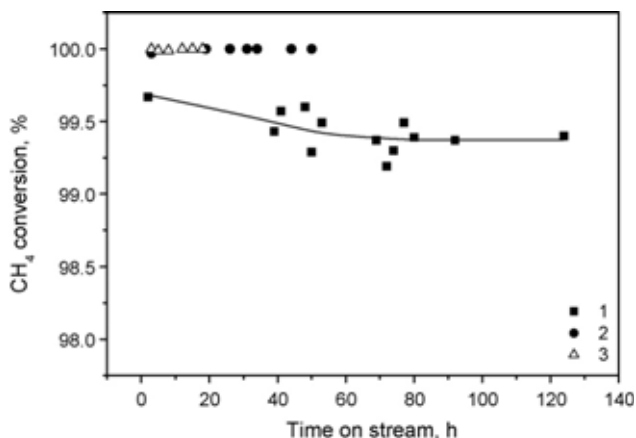
Fig. 6. Methane conversion vs. operation time in CCC for different catalyst packages: (1) uniform catalyst package Pd–Mn–La–Al$_2$O$_3$, rings (T_{in} = 575–580 ◦C, GHSV= 15, 100 h^{-1}, α= 6.8-6.9); (2) combined catalyst package: Pd–Mn–La–Al$_2$O$_3$, rings and spheres (Tin = 575–580 ◦C, GHSV= 12,500 h^{-1}, α = 6.7–6.8); (3) combined catalyst package: Mn–La–Al$_2$O$_3$, rings, and Pd–Mn–La–Al$_2$O$_3$, spheres (T_{in} – 575–580◦C, GHSV= 12,500 h^{-1}, α = 6.7–6.8).
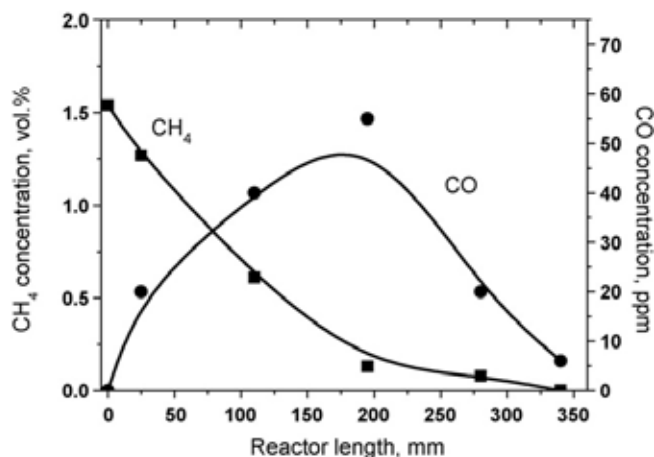
Fig. 7. Profiles of methane and CO concentrations along the reactor length during combustion of natural gas on a combined catalyst package Pd–Mn–La–Al$_2$O$_3$: 280 mm of rings and 60 mm of spherical granules (T$_{in}$ = 580 ∘C, GHSV= 12,500 h^{-1}).

the catalyst package, i.e. in the area where the spherical catalyst is loaded. The layer of this catalyst has a higher density and higher geometrical area, which provides more efficient use of the catalyst, and thus increases the CCC efficiency.

Then, we determined the role of catalyst activity in the total CCC efficiency. We carried out tests on a combined catalyst package consisting on Mn–La–Al$_2$O$_3$ (rings) and Pd–Mn–La–Al$_2$O$_3$ (spheres) and compared the methane conversion with the results of the previous test. The ratio of the layer heights was similar to that used in the previous test – 280/60mm. The total Pd content in CCC was much lower - about 0.1 wt.% because most of the catalyst package consisted of the Mn–La–Al$_2$O$_3$ catalyst. The activity of this catalyst (T$_{50\%\ CH4}$) is lower than that of Pd–Mn–La–Al$_2$O$_3$ (Table 3). However, the substitution of the more active catalyst with a less active and a 6-fold decrease of the total Pd content (Fig. 6, curve 3) did not decrease the methane combustion efficiency compared to the previous test (Fig. 6, curve 2) where the total Pd content was 0.6 wt.%. Thus, increase of the efficiency of the use of the catalyst granules even at a relatively short length of the CCC results in a noticeable improvement of the overall CCC efficiency at a low total Pd loading.

However, such CCC design produced a larger pressure drop than the uniform catalyst package with ring-shaped catalysts. The pressure drop in the two-stage catalyst package was 48 mbar at GHSV= 12,500 h^{-1} and 30 mbar at GHSV= 10,000 h^{-1}. The pressure drop in the layer of the spherical Pd–Mn–La–Al$_2$O$_3$ catalyst was 20 and 13 mbar, respectively.

The tests of CCC with a combined two-stage catalyst package at lower inlet temperature showed that the inlet temperature decrease from 580 to 470 ∘C decreased the methane combustion efficiency. The methane conversion over the catalyst package Pd–Mn–La–Al$_2$O$_3$ (rings)/Pd–Mn–La–Al$_2$O$_3$ (spheres) decreased from 99.93% to 99.7% with methane and CO concentrations increasing to 37 and 150 ppm, respectively. The methane conversion over the catalyst package Mn–La–Al$_2$O$_3$ (rings)/Pd–Mn–La–Al$_2$O$_3$ (spheres) at the inlet temperature

470 $\circ$C was only 99.4% with methane and CO concentrations 90 and 220 ppm, respectively. The increase of the methane combustion efficiency at low inlet temperature was made possible by organizing a three-stage catalyst package.

5.4 Tests of CCC with combined three-stage catalyst package

In the three-stage catalyst package we placed a highly active Pd–Ce–Al_2O_3 catalyst with 2 wt.% Pd at the entrance zone. Most of the package consisted of Mn–La–Al_2O_3 catalyst. Both catalysts were shaped as 7.5 mm × 7.5 mm × 2.5 mm rings. Pd–Mn–La–Al_2O_3 catalyst in the form of 4–5 mm spherical granules was placed in the downstream part of the catalyst package. The ratio of the catalyst layer heights was 40/240/60mm. Similarly to the tests of two-stage packages, the ratio of the heights of ring and spherical granules was 280/60mm. The tests were carried out at the inlet temperature 470 $\circ$C, GHSV= 10,000 h^{-1} and α = 5.2. Under such conditions the temperature at the outlet zone of the catalyst package remained at about 950 $\circ$C.

Figure 8a shows the temperature profile along the CCC length. In the inlet zone filled with the Pd–Ce–Al_2O_3 catalyst at 25 mm from the inlet the feed is heated from 470 to 580 $\circ$C due to catalytic combustion of methane. The latter temperature is sufficiently high for effective functioning of the main Mn–La–Al_2O_3 catalyst bed. Further temperature growth from 580 to 950$\circ$C takes place on this catalyst.

The profiles of the methane and CO concentrations along the CCC length are shown in Fig. 8b. The methane concentration profile shows a sharp concentration fall in the inlet zone where the Pd–Ce–Al_2O_3 catalyst is located. The main decrease of the concentration from 1.4% to 170 ppm takes place in the zone of the main catalyst Mn–La–Al_2O_3 (40–280 mm). Then at the CCC exit in the layer of the spherical Pd–Mn–La–Al_2O_3 catalyst the residual amounts of methane burn from 170 to 0–10 ppm concentrations. The concentration of the CO intermediate initially grows. Then, when most methane is oxidized, the CO concentration also decreases from 300 to 40 ppm in the Mn–La–Al_2O_3 bed. Finally, residual CO is burned in the spherical Pd–Mn–La–Al_2O_3 catalyst to 10 ppm concentrations. The pressure drop in the catalyst package was 29–30 mbar.

Thus, the use of the three-stage combined catalyst package including a thin layer of the active palladium–ceria catalyst located at the CCC entrance before the main oxide catalyst bed allows us to increase the CCC efficiency for methane combustion and obtain required low methane emission value of 10 ppm at low inlet temperature 470$\circ$C. This additional catalyst layer provides the initial methane conversion and temperature increase before the main catalyst bed.

6. Modeling of methane combustion processes in a catalytic combustor

6.1 Model description

The catalytic packages used in modeling are schematically presented in Fig. 3. For calculation of the catalyst package performance, we used a model of a steady-state adiabatic plug-flow reactor. The calculation of the temperature profiles and methane conversion was performed at variation of catalyst methane oxidation activity and geometry of catalyst granules, ratio of bed lengths of different catalysts in the package, temperature, pressure and gas space velocity in the combustor.
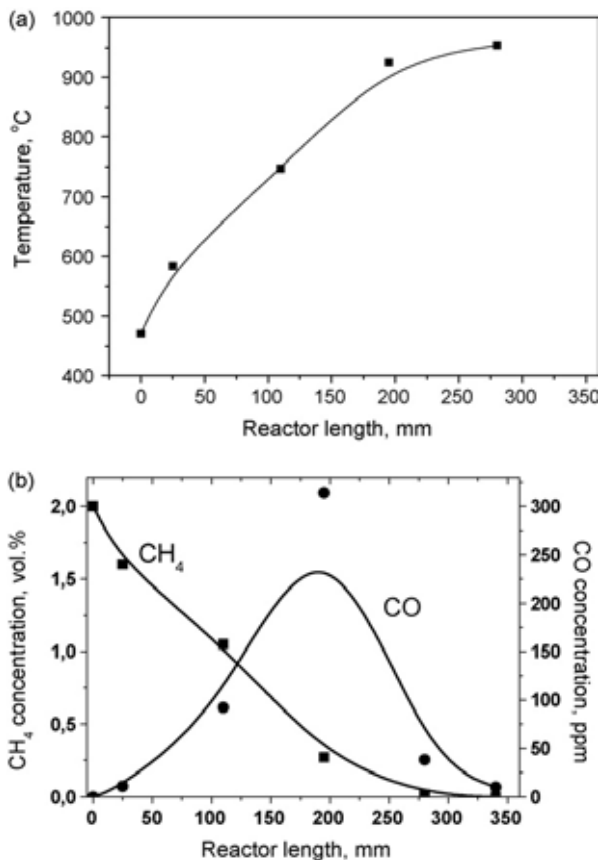
Fig. 8. Profiles of temperature (a) and methane and CO concentrations (b) along the reactor length during combustion of natural gas on a combined catalyst package Pd–Mn–La–Al$_2$O$_3$/Mn–La–Al$_2$O$_3$/Pd–Ce–Al$_2$O$_3$ (T_{in} = 470 °C, GHSV= 10,000 h^{-1}, α = 5.2).

The reaction rate was calculated using Eqs. (1) and (2):

$$W = k\, C_{CH_4} \left(\frac{P}{P_0} \right) \qquad (1)$$

$$k = \eta\, k_0 (1-\varepsilon) \exp\left(-\frac{E/R}{T} \right) \qquad (2)$$

where k is the kinetic constant (s^{-1}), C$_{CH4}$ is the methane concentration (molar fraction), P is the operating pressure (bar), P$_0$ is the pressure (bar) at which the reaction kinetics is studied experimentally (in this case it is equal to 1 bar), η is efficiency factor (dimensionless), k$_0$ is the pre-exponential factor of the kinetic constant (s^{-1}), E is the activation energy (J mol^{-1}), R is the univeral gas constant (J mol^{-1}K^{-1}), ε is the fractional void volume in the catalyst bed (dimensionless).

Thank You for previewing this eBook

You can read the full version of this eBook in different formats:

➢ HTML (Free /Available to everyone)

➢ PDF / TXT (Available to V.I.P. members. Free Standard members can access up to 5 PDF/TXT eBooks per month each month)

➢ Epub & Mobipocket (Exclusive to V.I.P. members)

To download this full book, simply select the format you desire below